

Antiferromagnetic spin- $\frac{1}{2}$ chains in (NO)Cu(NO₃)₃: A microscopic studyO. Janson,* A. A. Tsirlin,[†] and H. Rosner[‡]*Max-Planck-Institut für Chemische Physik fester Stoffe, D-01187 Dresden, Germany*

(Received 6 July 2010; published 9 November 2010)

We report on the microscopic model of the recently synthesized one-dimensional quantum magnet (NO)Cu(NO₃)₃. Applying density-functional-theory band-structure calculations, we obtain a leading antiferromagnetic exchange coupling $J \approx 200$ K, which runs via NO₃ groups forming spin chains along the b direction. Much weaker couplings $J' \approx 2$ K link the chains into layers in a nonfrustrated manner. Our calculations do not support the earlier conjecture on an anisotropic frustrated square lattice physics in (NO)Cu(NO₃)₃. In contrast, the model of uniform spin chains leads to a remarkably good fit of the experimental magnetic susceptibility data, although the low-temperature features of the intrinsic magnetic susceptibility measured by electron spin resonance might call for extension of the model. We outline possible experiments to observe the suggested long-range magnetic ordering in (NO)Cu(NO₃)₃ and briefly compare this compound to other spin- $\frac{1}{2}$ uniform-chain systems.

DOI: 10.1103/PhysRevB.82.184410

PACS number(s): 75.30.Et, 71.20.Ps, 75.10.Pq, 75.10.Jm

Quantum magnets give an exciting opportunity to observe unusual ground states and to establish unexpected connections between theoretical models and real systems.^{1,2} Quantum spin chains are in the focus of numerous recent studies and show peculiar excitation spectra³ along with the promising effect of the ballistic heat transport.⁴ Among the spin-chain models, the properties of the uniform spin chain are now well understood theoretically and extensively verified experimentally via versatile investigations for a range of model compounds.^{3,5–7} The crucial present-day task is to extend these results to other systems with different dimensionality, different lattice topologies, and, consequently, different physics. One of the possible approaches to this challenging problem is to explore compounds with unusual chemical features that can lead to peculiar crystal structures and spin lattices. Yet, the deduction of the correct spin model for a complex crystal structure will often require a microscopic study to provide quantitative estimates of the individual exchange couplings.

The (NO)Cu(NO₃)₃ compound⁸ is one of the recent examples for a low-dimensional magnet with a special chemical feature, the nitrosonium [NO]⁺ cation that forms a mixed salt with the magnetic spin- $\frac{1}{2}$ Cu²⁺. The peculiar crystal structure (Fig. 1) is formed by chains of isolated CuO₄ plaquettes running along the b direction. One type of the triangular [NO₃][−] nitrate anions links the plaquettes within a chain, thus connecting to two neighboring plaquettes. The nitrate groups of the second type are connected to one plaquette only. The chains stack along the a and c directions whereas the [NO]⁺ cations are found between the chains. The crystal symmetry is monoclinic (space group $P2_1/m$).

An experimental study⁹ of (NO)Cu(NO₃)₃ evidenced low-dimensional spin correlations and proposed a two-dimensional Nersesyan-Tsvetlik model¹⁰ which is better known as an anisotropic frustrated square lattice.¹¹ Based on phenomenological arguments, in particular, (i) the almost temperature-independent values of the g factor and (ii) the lack of sharp anomalies in the specific heat, the absence of long-range ordering (LRO) at least down to 2 K is proposed.⁹ At the same time, the experimental magnetic susceptibility

evidences that the leading magnetic exchange coupling J (along the structural chains, Fig. 1) exceeds 150 K. To reconcile the large coupling with the absence of LRO, the authors of Ref. 9 suggest that the interchain couplings J' and J_2 in the (NO)Cu(NO₃)₃ structure show an exactly 2:1 ratio (see Fig. 1), thus leading to strong frustration that inhibits LRO.

Since individual exchange couplings are not directly measurable, it is generally difficult to judge whether a specific system is magnetically frustrated or not. For instance, such discussion for the spin- $\frac{1}{2}$ diamond chain system azurite Cu₃(CO₃)₂(OH)₂ (Ref. 12) is still not settled: while inelastic neutron-scattering data favor nonfrustrated magnetism,¹³ band-structure calculations suggest a frustrated model,^{14,15} whereas thermodynamical data can be satisfactorily described by both models.^{15,16} Even more illustrative is the recent evidence¹⁷ of a nonfrustrated spin model in (CuCl)LaNb₂O₇, initially proposed to imply magnetism of the frustrated square lattice.¹⁸

Moreover, the conjecture on the exact $J_2:J'=1:2$ ratio in (NO)Cu(NO₃)₃ is based on two nontrivial assumptions: (i) the J_2 and J' couplings are running exclusively via NO groups; (ii) the energies of these couplings are proportional to the number of bridging NO units (two for J' and one for J_2).⁹ Regarding the complexity of exchange interactions in general, such assumptions should be supported by a microscopic verification. Band-structure calculations are known as a reliable and accurate tool to investigate magnetism on the microscopic level.^{19–22} In particular, this method has been successfully applied to frustrated square lattice systems²³ and to a variety of Cu²⁺ compounds.^{7,20,24} Therefore, we perform band-structure calculations and evaluate individual exchange couplings in (NO)Cu(NO₃)₃. We find that the simple counting of the bridging [NO]⁺ groups is an inappropriate approach because it does not regard the different geometry of the superexchange pathways.²⁵ Our calculations describe (NO)Cu(NO₃)₃ as an essentially one-dimensional (1D) and nonfrustrated system. This conflicting finding calls for reconsideration of the available experimental data.

The scalar-relativistic density-functional-theory (DFT)

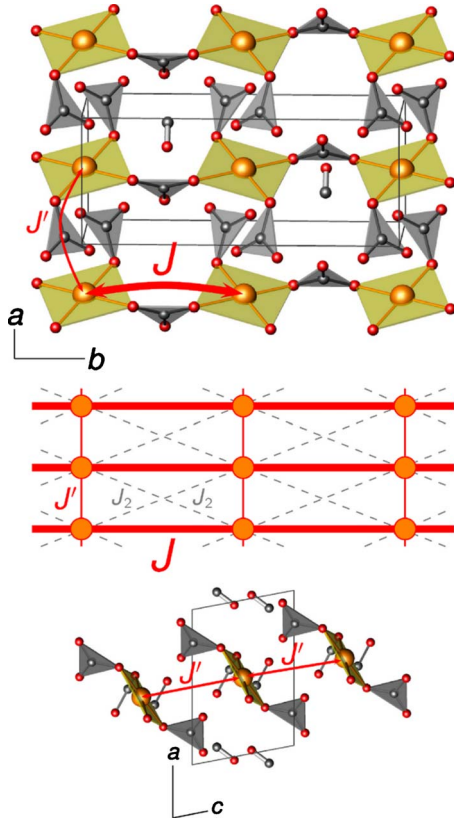


FIG. 1. (Color online) Crystal structure (top and bottom) and the spin model (middle) of $(\text{NO})\text{Cu}(\text{NO}_3)_3$. The neighboring CuO_4 plaquettes are connected via NO_3 triangles and form chains along b (top). The chains are well separated by $[\text{NO}]^+$ cations (bottom). In the top panel, the nearly overlapping NO_3 triangles lie in different planes and remain *disconnected* (see also the bottom panel).

calculations were performed using the full-potential FPLO9.00-33 code.^{26,27} For the local-density approximation (LDA), the Perdew-Wang parametrization²⁸ of the exchange-correlation potential was chosen. LDA calculations were done on a converged mesh of 1920 k points (588 points in the irreducible wedge).

LDA is known to fail describing the insulating properties of cuprates. Nevertheless, it provides reliable information on the relevant orbitals and leading antiferromagnetic (AFM) exchange couplings. Among others, magnetic excitations have the smallest energy, and essentials of magnetism are concealed in the close vicinity of the Fermi level ϵ_F . A sharp peak of NO states appearing at 1 eV above ϵ_F is a peculiar feature of $(\text{NO})\text{Cu}(\text{NO}_3)_3$ related to the antibonding π^* states of the $[\text{NO}]^+$ cation (two nearly degenerate orbitals for each NO group). In other respects, the valence band of $(\text{NO})\text{Cu}(\text{NO}_3)_3$ comprises features typical for cuprates: it has a width of about 5 eV and consists predominantly of Cu $3d$ and O $2p$ states (Fig. 2). The well-separated density of states for the antibonding Cu-O bands at ϵ_F has two distinct maxima (Van Hove singularities), characteristic of a 1D behavior. Assuming the simplest nearest-neighbor chain scenario, the width W of the antibonding band readily yields the leading hopping term $t=W/4 \approx 180$ meV.

To account for all the possible exchange couplings in

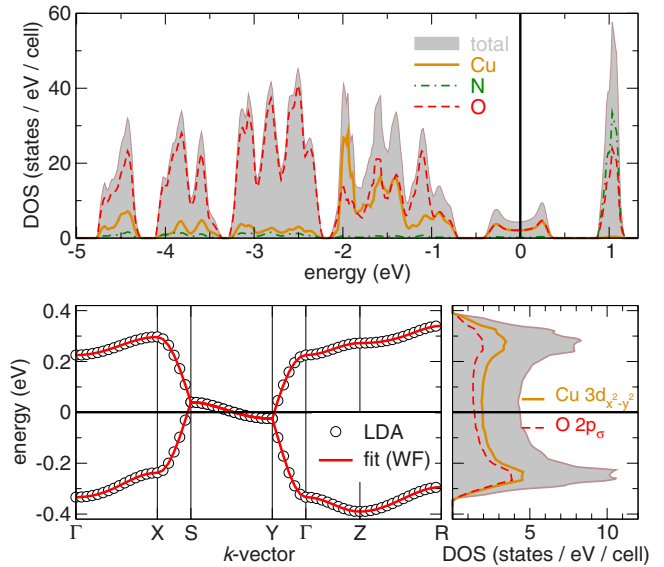


FIG. 2. (Color online) Top: the valence band of $(\text{NO})\text{Cu}(\text{NO}_3)_3$. The Fermi level ϵ_F is at zero energy. Bottom left: the band structure of the two-band $d\rho$ complex at ϵ_F and the fit using the Wannier functions technique. Bottom right: the orbital-resolved density of states for the antibonding band.

$(\text{NO})\text{Cu}(\text{NO}_3)_3$, we consider the valence bands in more detail. The two-band complex at ϵ_F is formed by σ overlapping Cu $3d_{x^2-y^2}$ and O $2p_{x,y}$ orbitals (Fig. 2, bottom right). The strong hybridization of these orbitals allows to treat them within an effective one-orbital model. The band structure (Fig. 2, bottom left) exhibits the predominant dispersion along X-S and Y- Γ . This corresponds to the crystallographic b direction and supports the proposed 1D scenario. To evaluate the hopping terms, we fit the valence bands using Wannier functions (WFs) (Ref. 29) based on Cu $3d_{x^2-y^2}$ states (Fig. 3).³⁰ The perfect fit to the LDA band structure (Fig. 2, bottom) justifies the WF procedure. This way, we obtain $t = 150$ meV for the leading nearest-neighbor intrachain hopping and a small nonfrustrated interchain hopping $t' = 17$ meV (Fig. 1, middle). Other hoppings are below 10 meV. In particular, the previously proposed t_2 (see Fig. 1) appeared to be as small as 2 meV, disfavoring the model with the frustrated interchain couplings. The couplings J and J' form layers whereas the leading hopping in the perpendicular direction is $t_{\perp} = 6$ meV.

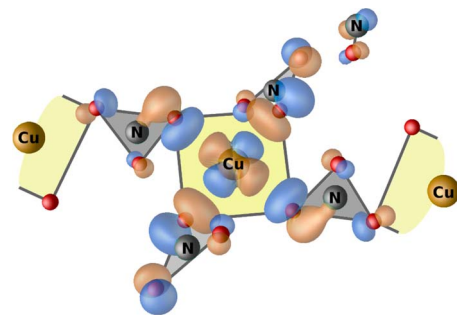


FIG. 3. (Color online) Fragment of the Heisenberg chain. The Wannier function for the Cu $3d_{x^2-y^2}$ orbital is shown.

In contrast to the apparent insulating behavior of (NO)Cu(NO₃)₃ evidenced by the blue color of the crystals,⁹ LDA yields a metallic ground state. This shortcoming of LDA originates from the well-known underestimate of strong electronic correlations, intrinsic for the 3d⁹ configuration of the magnetic Cu⁺² ions. To restore the insulating ground state, we add the missing part of correlations in two ways: (i) by mapping the LDA band structure onto a Hubbard model; (ii) by treating the correlations in a mean-field way via the local spin-density approximation plus U approach (LSDA+ U) with the around-mean-field double-counting-correction scheme.

Adopting the mapping procedure, we transfer the leading hoppings onto a Hubbard model with the effective on-site Coulomb repulsion U_{eff} . Here, the low-energy excitations can be described by a Heisenberg model since the $t \ll U_{\text{eff}}$ condition and the half-filling regime are both well justified for undoped cuprates.³¹ Assuming a typical value of $U_{\text{eff}}=4.5$ eV,^{24,32,33} we readily obtain the AFM part of the exchange integrals using the expression of second-order perturbation theory $J_i^{\text{AFM}}=4t_i^2/U_{\text{eff}}$. This way, we find $J^{\text{AFM}}=230$ K and $J'^{\text{AFM}}=3$ K. The frustrating coupling $J_2^{\text{AFM}} \approx 0.04$ K is negligible. The interlayer coupling is $J_{\perp}=0.4$ K.

As an alternative approach, we apply the LSDA+ U scheme to evaluate J and J' since long-range terms are negligible as demonstrated above. The similarity of (NO)Cu(NO₃)₃ to other Cu⁺² oxides allows to adopt the typical values of the Coulomb repulsion and exchange parameters $U_d=6.5 \pm 1$ eV and $J_d=1$ eV, respectively.³⁴ This parameter set yields accurate estimates of individual exchange couplings for related Cu⁺² compounds.^{24,32,33} For (NO)Cu(NO₃)₃, we obtain the insulating ground state (band gap $E_g=1.7$ eV) with exchange couplings $J=200 \mp 50$ K and J' below 1 K. Therefore, the model and the LSDA+ U approaches consistently describe (NO)Cu(NO₃)₃ as a 1D system with the leading exchange coupling of about 200 K and the interchain coupling below 3 K.

The interchain coupling J' likely runs via the NO groups, as evidenced by small tails of π^* NO molecular orbitals in the Cu-based WFs (Fig. 3). Nevertheless, the hoppings depend on the mutual orientation of the WFs, hence a simple counting of the bridging NO units neglects a basic ingredient of the superexchange mechanism. In contrast, our extensive DFT calculations suggest $J_2 \ll J'$ and do not support the earlier conjecture on the exact $J'/J_2=2:1$ ratio.⁹ In conflict with Ref. 9, we find that (NO)Cu(NO₃)₃ is an essentially nonfrustrated 1D spin system. It is rather similar to other 1D Cu⁺² compounds with CuO₄ plaquettes separated by nonmagnetic groups. The J value of 150–250 K is typical for the Cu-O-O-Cu superexchange, e.g., in the uniform-spin-chain compounds $M_2\text{Cu}(\text{PO}_4)_2$ ($M=\text{Sr}$ and Ba).²⁴

In the following, we reconsider the experimental data for (NO)Cu(NO₃)₃ in light of the nonfrustrated 1D spin model suggested by the DFT calculations. We first discuss magnetic susceptibility. The susceptibility curves were computed via quantum Monte Carlo (QMC) method using the loop³⁵ and worm algorithms, implemented in the ALPS simulation package.³⁶ We performed simulations for finite lattices with periodic boundary conditions. The typical lattice size was

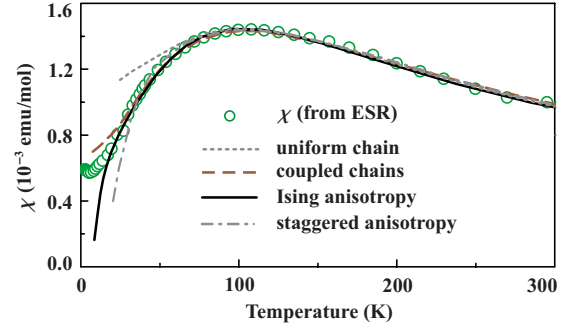


FIG. 4. (Color online) Magnetic susceptibility (χ) of (NO)Cu(NO₃)₃ compared to different spin models: the uniform spin chain, coupled uniform chains, the uniform chain with Ising anisotropy [Eq. (1)], and the uniform chain with staggered anisotropy [Eq. (2), $\tilde{\Delta}=0$], see text for details. Experimental data are the scaled ESR intensities from Ref. 9.

$N=60-100$ for 1D models and $N=1500-2000$ for the model of coupled spin chains. Calculations for lattices of different size showed negligible finite-size effects for the temperature range considered. Regarding the experimental data, we first discuss the temperature dependence of the electron spin resonance (ESR) intensity that can be taken as a direct measure of χ .⁹

The ESR data show a broad maximum at $T_{\text{max}}^{\chi} \approx 100$ K. In the uniform-spin-chain model, $T_{\text{max}}^{\chi} \approx 0.64J$,³⁷ hence $J \approx 156$ K. This value is in good agreement with our DFT estimate of 150–250 K. However, the uniform-chain fit overestimates the susceptibility below 80 K (Fig. 4). To improve the fit in the low-temperature region, several extensions/modifications of the uniform-chain model are suggested.

First, the interchain coupling J' reduces quantum fluctuations, thus leading to a lower magnetic susceptibility at low temperatures. Indeed, we found a good fit of the experimental data down to 30 K with $J'/J=0.4$, $J=150$ K, and $g=2.13$ (dashed line in Fig. 4). The value of J' is, however, far too large compared to the DFT estimate of $J'/J \approx 0.01$.

At present, DFT calculations can provide reliable numerical estimates only for the case of isotropic (Heisenberg) couplings. Therefore, anisotropic effects should be considered “on top” of the isotropic, DFT-based model. Various simulation techniques (e.g., QMC) are capable of including the anisotropy, thereby offering a possibility of a direct comparison to experiments.

The symmetric (Ising/ XY) anisotropy³⁸

$$\hat{H} = J \sum_{\langle ij \rangle} [S_i^x S_j^x + S_i^y S_j^y + (1 + \Delta) S_i^z S_j^z] \quad (1)$$

has pronounced effect on the low-temperature part of the susceptibility curve. In particular, the Ising anisotropy ($\Delta > 0$) opens a spin gap and reduces the low-temperature susceptibility. Thus, we are able to fit the data down to 20 K with $J=95$ K, $\Delta=1$, and $g=2.07$ (solid line in Fig. 4). Since experimental data for other Cu⁺² compounds suggest $\Delta \leq 0.2$ (Refs. 39 and 40), the fitted value of $\Delta=1$ looks rather overestimated.

Other anisotropy effects are the g -tensor anisotropy and the antisymmetric Dzyaloshinskii-Moriya (DM) exchange. Owing to the $P2_1/m$ symmetry of the $(\text{NO})\text{Cu}(\text{NO}_3)_3$ structure, the neighboring Cu atoms are imaged with the 2_1 screw axis, leading to the possible staggered anisotropy of the g tensor (according to Ref. 9, there is a sizable difference between the g -tensor components: $g_{\parallel}=2.06$ and $g_{\perp}=2.36$). The mirror planes are perpendicular to the b axis and run between the neighboring Cu atoms, thus confining the DM vector to be perpendicular to the b axis (i.e., to lie within the ac plane). Further on, the 2_1 screw axis induces opposite DM vectors on the neighboring bonds and leads to their staggered configuration. Following the general framework developed in Ref. 41, we describe the uniform chain with staggered anisotropy using the Hamiltonian

$$\hat{H} = J \sum_{\langle ij \rangle} [S_i^x S_j^x + S_i^y S_j^y + (1 + \tilde{\Delta}) S_i^z S_j^z] - h_u \sum_i S_i^x - h_s \sum_i (-1)^i S_i^z, \quad (2)$$

where the first term is the bilinear exchange with the symmetric anisotropy $\tilde{\Delta}$ [i.e., Δ from Eq. (1) modified by the staggered anisotropy]. The effective uniform (h_u) and staggered (h_s) fields depend on the applied external field (H) and on the staggered anisotropy.

The general effect of the staggered anisotropy is the opening of a spin gap and thus a reduction in the low-temperature susceptibility for certain directions of the applied field.⁴¹ At fixed $\tilde{\Delta}$, the gap mainly depends on h_s . For simplicity, we fix $\tilde{\Delta}=0$ and fit the data down to 25 K with $h_s/J=0.15$, $J=160$ K, and $g=2.06$. The uniform component of the field can be varied in a wide range, thus leaving freedom for H and the staggered anisotropy parameters.⁴² Since $h_s=H \sin \frac{\alpha}{2}$ and $\tan \alpha=|\mathbf{D}|/J$ (Ref. 41), we find $H/J \geq 0.13$ that definitely exceeds the typical field value of 0.3 T in an X-band ESR experiment. The $|\mathbf{D}|$ value is effective and implicitly contains the staggered anisotropy of the g tensor which is presently unknown.

We conclude that none of the anisotropy parameters can be taken as a sole reason for the reduced susceptibility at low temperatures. However, the combination of different anisotropies slightly improves the situation and brings the numbers closer to our expectations: $\tilde{\Delta}=0.5$ and $h_s/J=0.06$ (dashed line in Fig. 5). Nevertheless, the presence of such a strong exchange anisotropy has to be challenged experimentally.

Weak dimerization might be an alternative to the exchange anisotropy. Since exchange couplings are highly sensitive to details of the crystal structure, a weak structural change will readily open the gap and reduce the susceptibility owing to the alternation of the exchange couplings along the chain. Experimental data are well fitted by an alternating $J-J''$ model³⁷ with $J=176$ K, the alternation ratio $J''/J=0.87$, and $g=2.10$ (solid line in Fig. 5). Although the available structural data do not suggest the dimerization, we are not aware of any structural studies below 160 K. More-

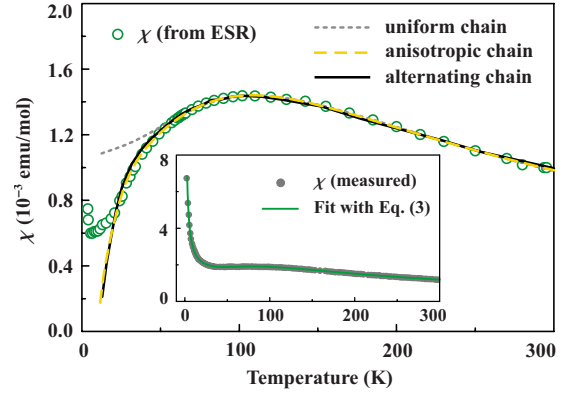


FIG. 5. (Color online) Same as Fig. 4 for the uniform spin chain, the anisotropic spin chain [Eq. (2), $\tilde{\Delta}=0.5$, $h_s/J=0.06$], and the alternating spin chain. The inset shows bulk susceptibility (Ref. 9) and the fit with Eq. (3). See text for details.

over, the nontrivial temperature dependence of the ESR linewidth⁹ might also be related to a structural change.

Trying to get further support for one of the above (rather speculative) scenarios, we consider other experimental data. Specific heat was reported in a narrow temperature range only (1.8–10 K).⁹ It shows a minimum around 5 K with an increase toward lower temperatures interpreted as a Schottky anomaly (although the characteristic maximum was not observed) and a typical increase toward higher temperatures due to the phonon contribution which is cubic in T . Since $J \approx 150$ K, the magnetic specific heat will show a maximum around 70 K,³⁷ hence the experimental data in this temperature range (along with the proper nonmagnetic reference to estimate the phonon contribution) could be helpful. Regarding the Schottky anomaly, no indication of its intrinsic origin has been given.⁹

In contrast to the specific heat, the raw magnetic susceptibility data are very instructive. Owing to the huge impurity contribution, the susceptibility maximum around 100 K is hardly visible. This situation is very typical for spin-chain systems, since 1D magnets are highly sensitive to impurities (a single defect breaks the chain).²⁴ Following previous studies,⁴³ we fit the data using the expression

$$\chi(T) = \chi_0 + C_{\text{imp}}/T + \chi_{\text{chain}}(T), \quad (3)$$

where χ_0 accounts for core diamagnetism and Van Vleck paramagnetism, C_{imp}/T is the Curie law to fit the impurity contribution, and $\chi_{\text{chain}}(T)$ is the susceptibility of the uniform spin chain.³⁷ We find a remarkably good fit down to 2 K with $\chi_0=7.7 \times 10^{-5}$ emu/mol, $C_{\text{imp}}=0.015$ emu K/mol (4% of spin- $\frac{1}{2}$ impurities), $J=150$ K, and $g=2.12$. Since the same model poorly fits the intrinsic susceptibility from ESR below 80 K (see Fig. 4), we are left with two options: (i) the impurity contribution is not properly described with the Curie law (then, the origin of this unusual “impurity” contribution is worth to unravel) or (ii) the ESR bears a systematic error that causes the underestimate of χ at low temperatures (probably, due to the separation of the intrinsic and impurity signals in the spectra). To resolve this puzzling issue, additional experimental studies, such as susceptibility measurements on

single crystals or nuclear magnetic resonance, are highly desirable.

Finally, we would like to comment on the possible LRO in (NO)Cu(NO₃)₃. Although Ref. 9 claims the absence of the LRO down to 2 K, we suggest a different estimate of $T_N < 5$ K since the upturn of the specific heat (Schottky anomaly) may conceal the expected weak transition anomaly below 5 K. The weakness of the anomaly is a natural consequence of $T_N \ll J$, which results in a significantly small amount of entropy released at T_N . Further on, ESR intensities diverge below 10 K and might also indicate the onset of LRO. Our upper estimate of $T_N = 5$ K corresponds to $T_N/J = 0.03$. We will show that such a low T_N is typical for a 1D system and should not be taken as a sole evidence of magnetic frustration.

In (NO)Cu(NO₃)₃, uniform spin chains with $J \approx 150$ K are coupled by $J'/J \approx 0.01$ and $J_{\perp}/J \approx 0.0025$. Unfortunately, the case of spatially anisotropic interchain couplings has not been considered theoretically, yet. Assuming the same interchain coupling $J'/J \approx 0.01$ along the two directions, we arrive at $T_N/J = 0.021$ (Ref. 44) which is already below our upper estimate of 0.03.⁴⁵ With proper accounting for the spatial anisotropy, T_N should be even lower because it is largely determined by the lowest interchain coupling J_{\perp} as the main obstacle for LRO. We conclude that the lack of clear observation of LRO in (NO)Cu(NO₃)₃ results from the pronounced one-dimensionality of the system. The low T_N does not evidence the strong frustration. Moreover, the DFT-based model approach accounts for all isotropic exchange couplings and does not show the frustration.

The low T_N in (NO)Cu(NO₃)₃ can be compared to other spin- $\frac{1}{2}$ uniform-chain magnets. Weak interchain couplings of $J'/J \approx 0.01$ were previously observed in Sr₂CuO₃ (Refs. 7 and 46) and Sr₂Cu(PO₄)₂ (Refs. 24 and 47). In these

compounds, the magnetic ordering temperatures are $T_N/J \approx 2 \times 10^{-3}$ and 5×10^{-4} , respectively, thus an ordering temperature of (NO)Cu(NO₃)₃ should be quite low and may even lie below 2 K ($\sim 10^{-2}J$).

In summary, DFT calculations suggest a consistent description of (NO)Cu(NO₃)₃ as a uniform-spin-chain system with weak and nonfrustrated interchain couplings. The magnetic ordering temperature T_N/J is predicted to be below 0.03, indicating that LRO could not be observed in previous experiments. To find experimental signatures of the LRO, low-temperature studies and sensitive experimental techniques (such as muon spin relaxation) should be applied. Regarding the behavior above T_N , the bulk magnetic-susceptibility data follow the uniform-chain model, whereas the intrinsic magnetic susceptibility measured by ESR shows lower χ below 80 K. We note that other spin-chain systems also reveal puzzling behavior at low temperatures. For example, Ref. 48 reports a complex ESR spectrum of (6MAP)CuCl₃ which was previously known as a uniform-spin-chain compound. To explain the experimental spectrum, the authors of Ref. 48 had to consider a spin chain with several inequivalent exchange couplings, although the structural data did not show any signatures of the distortion. It is possible that numerous systems, assigned to the uniform-chain model from bulk magnetic-susceptibility measurements, are more complex than they appear. Further studies should shed light to this problem.

We are grateful to Alexander Vasiliev, Olga Volkova, Olivier Cépas, and Philippe Sindzingre for stimulating our interest to (NO)Cu(NO₃)₃ and fruitful discussions. We thank Vladislav Kataev for providing us with the numerical data on ESR intensities. A.A.T. was funded by Alexander von Humboldt Foundation.

*janson@cpfs.mpg.de

†altsirlin@gmail.com

‡rosner@cpfs.mpg.de

¹T. Giamarchi, C. Rüegg, and O. Tchernyshyov, *Nat. Phys.* **4**, 198 (2008).

²M. Klanjšek, H. Mayaffre, C. Berthier, M. Horvatić, B. Chiari, O. Piovesana, P. Bouillot, C. Kollath, E. Orignac, R. Citro, and T. Giamarchi, *Phys. Rev. Lett.* **101**, 137207 (2008).

³M. B. Stone, D. H. Reich, C. Broholm, K. Lefmann, C. Rischel, C. P. Landee, and M. M. Turnbull, *Phys. Rev. Lett.* **91**, 037205 (2003).

⁴A. V. Sologubenko, K. Berggold, T. Lorenz, A. Rosch, E. Shimshoni, M. D. Phillips, and M. M. Turnbull, *Phys. Rev. Lett.* **98**, 107201 (2007).

⁵B. Lake, D. A. Tennant, C. D. Frost, and S. E. Nagler, *Nature Mater.* **4**, 329 (2005).

⁶M. Takigawa, N. Motoyama, H. Eisaki, and S. Uchida, *Phys. Rev. Lett.* **76**, 4612 (1996).

⁷H. Rosner, H. Eschrig, R. Hayn, S.-L. Drechsler, and J. Málek, *Phys. Rev. B* **56**, 3402 (1997).

⁸K. O. Znamenkov, I. V. Morozov, and S. I. Troyanov, *Russ. J. Inorg. Chem.* **49**, 172 (2004).

⁹O. Volkova, I. Morozov, V. Shutov, E. Lapsheva, P. Sindzingre, O. Cépas, M. Yehia, V. Kataev, R. Klingeler, B. Büchner, and A. Vasiliev, *Phys. Rev. B* **82**, 054413 (2010).

¹⁰A. A. Nersesyan and A. M. Tselvik, *Phys. Rev. B* **67**, 024422 (2003).

¹¹For example, O. A. Starykh and L. Balents, *Phys. Rev. Lett.* **93**, 127202 (2004).

¹²H. Kikuchi, Y. Fujii, M. Chiba, S. Mitsudo, T. Idehara, T. Tonegawa, K. Okamoto, T. Sakai, T. Kuwai, and H. Ohta, *Phys. Rev. Lett.* **94**, 227201 (2005); B. Gu and G. Su, *ibid.* **97**, 089701 (2006); H. Kikuchi, Y. Fujii, M. Chiba, S. Mitsudo, T. Idehara, T. Tonegawa, K. Okamoto, T. Sakai, T. Kuwai, and H. Ohta, *ibid.* **97**, 089702 (2006).

¹³K. C. Rule, A. U. B. Wolter, S. Süllow, D. A. Tennant, A. Brühl, S. Köhler, B. Wolf, M. Lang, and J. Schreuer, *Phys. Rev. Lett.* **100**, 117202 (2008).

¹⁴J. Kang, C. Lee, R. K. Kremer, and M.-H. Whangbo, *J. Phys.: Condens. Matter* **21**, 392201 (2009).

¹⁵H. Jeschke, I. Opahle, H. Kandpal, R. Valentí, H. Das, T. Saha-Dasgupta, O. Janson, H. Rosner, A. Brühl, B. Wolf, M. Lang, J. Richter, S. Hu, X. Wang, R. Peters, T. Pruschke, and A. Honecker (unpublished).

- ¹⁶Y.-C. Li, *J. Appl. Phys.* **102**, 113907 (2007).
- ¹⁷A. A. Tsirlin and H. Rosner, *Phys. Rev. B* **82**, 060409 (2010).
- ¹⁸H. Kageyama, T. Kitano, N. Oba, M. Nishi, S. Nagai, K. Hirota, L. Viciu, J. B. Wiley, J. Yasuda, Y. Baba, Y. Ajiro, and K. Yoshimura, *J. Phys. Soc. Jpn.* **74**, 1702 (2005).
- ¹⁹D. J. Singh and I. I. Mazin, *Phys. Rev. B* **63**, 165101 (2001).
- ²⁰R. Valentí, T. Saha-Dasgupta, C. Gros, and H. Rosner, *Phys. Rev. B* **67**, 245110 (2003).
- ²¹V. V. Mazurenko, S. L. Skornyakov, V. I. Anisimov, and F. Mila, *Phys. Rev. B* **78**, 195110 (2008).
- ²²H. J. Xiang, E. J. Kan, S.-H. Wei, M.-H. Whangbo, and J. Yang, *Phys. Rev. B* **80**, 132408 (2009).
- ²³A. A. Tsirlin and H. Rosner, *Phys. Rev. B* **79**, 214417 (2009).
- ²⁴M. D. Johannes, J. Richter, S.-L. Drechsler, and H. Rosner, *Phys. Rev. B* **74**, 174435 (2006).
- ²⁵Following the argument of Ref. 9, one easily proves that the conventional 90° Cu-O-Cu superexchange is twice as large as the 180° superexchange (two and one Cu-O-Cu bridges, respectively).
- ²⁶K. Koepernik and H. Eschrig, *Phys. Rev. B* **59**, 1743 (1999).
- ²⁷In our calculations, we use the structural data at 160 K, as provided by A. Vasiliev and O. Volkova (private communication).
- ²⁸J. P. Perdew and Y. Wang, *Phys. Rev. B* **45**, 13244 (1992).
- ²⁹H. Eschrig and K. Koepernik, *Phys. Rev. B* **80**, 104503 (2009).
- ³⁰To ensure the validity of the effective one-orbital model, we considered an extended model which includes, in addition to the Cu $3d_{x^2-y^2}$ orbitals, NO orbitals lying ~ 1 eV above the Fermi level. The respective WF fit evidences that the hopping between Cu and NO orbitals is negligible and does not exceed 0.8 meV, justifying the one-orbital model.
- ³¹W. E. Pickett, *Rev. Mod. Phys.* **61**, 433 (1989).
- ³²O. Janson, R. O. Kuzian, S.-L. Drechsler, and H. Rosner, *Phys. Rev. B* **76**, 115119 (2007).
- ³³O. Janson, A. A. Tsirlin, M. Schmitt, and H. Rosner, *Phys. Rev. B* **82**, 014424 (2010).
- ³⁴The difference between U_{eff} and U_d is explained in Ref. 23.
- ³⁵S. Todo and K. Kato, *Phys. Rev. Lett.* **87**, 047203 (2001).
- ³⁶A. Albuquerque, F. Alet, P. Corboz, P. Dayal, A. Feiguin, S. Fuchs, L. Gamper, E. Gull, S. Gürtler, A. Honecker, R. Igarashi, M. Körner, A. Kozhevnikov, A. Läuchli, S. R. Manmana, M. Matsumoto, I. P. McCulloch, F. Michel, R. M. Noack, G. Pawłowski, L. Pollet, T. Pruschke, U. Schöllwöck, S. Todo, S. Trebst, M. Troyer, P. Werner, and S. Wessel, *J. Magn. Magn. Mater.* **310**, 1187 (2007).
- ³⁷D. C. Johnston, R. K. Kremer, M. Troyer, X. Wang, A. Klümper, S. L. Bud'ko, A. F. Panchula, and P. C. Canfield, *Phys. Rev. B* **61**, 9558 (2000).
- ³⁸Here, x , y , and z denote different components of the exchange that are, in general, unrelated to the local axes of the CuO_4 plaquette.
- ³⁹H.-A. Krug von Nidda, L. E. Svistov, M. V. Eremin, R. M. Eremina, A. Loidl, V. Kataev, A. Validov, A. Prokofiev, and W. Abmus, *Phys. Rev. B* **65**, 134445 (2002).
- ⁴⁰R. M. Eremina, M. V. Eremin, V. N. Glazkov, H.-A. Krug von Nidda, and A. Loidl, *Phys. Rev. B* **68**, 014417 (2003).
- ⁴¹M. Oshikawa and I. Affleck, *Phys. Rev. Lett.* **79**, 2883 (1997).
- ⁴²The magnetic susceptibility of the uniform chain with the staggered anisotropy should depend on the direction of the applied field. Unfortunately, Ref. 9 reports ESR measurements for two directions of the applied field only and does not allow to perform an extensive comparison with models involving the staggered anisotropy.
- ⁴³For example: A. Möller, M. Schmitt, W. Schnelle, T. Förster, and H. Rosner, *Phys. Rev. B* **80**, 125106 (2009).
- ⁴⁴C. Yasuda, S. Todo, K. Hukushima, F. Alet, M. Keller, M. Troyer, and H. Takayama, *Phys. Rev. Lett.* **94**, 217201 (2005).
- ⁴⁵The proposed Ising anisotropy $\tilde{\Delta}=0.5$ reduces quantum fluctuations and enhances T_N . To decide on the relevance of this effect, we evaluated T_N for a system of spin chains coupled by an effective interchain coupling $J_{\perp}^{\text{eff}}/J=0.05$. The chains with isotropic exchange order at $T_N/J=0.09$ (see also Ref. 44) whereas the Ising anisotropy $\tilde{\Delta}=0.5$ shifts the ordering temperature to $T_N/J=0.21$. Thus, the effect is rather strong but it does not influence any of our conclusions.
- ⁴⁶N. Motoyama, H. Eisaki, and S. Uchida, *Phys. Rev. Lett.* **76**, 3212 (1996); K. M. Kojima, Y. Fudamoto, M. Larkin, G. M. Luke, J. Merrin, B. Nachumi, Y. J. Uemura, N. Motoyama, H. Eisaki, S. Uchida, K. Yamada, Y. Endoh, S. Hosoya, B. J. Sternlieb, and G. Shirane, *ibid.* **78**, 1787 (1997).
- ⁴⁷A. Belik, S. Uji, T. Terashima, and E. Takayama-Muromachi, *J. Solid State Chem.* **178**, 3461 (2005).
- ⁴⁸M. Ozerov, A. A. Zvyagin, E. Čížmár, J. Wosnitza, R. Feyersherm, F. Xiao, C. P. Landee, and S. A. Zvyagin, *Phys. Rev. B* **82**, 014416 (2010).